[Downloaded free from http://www.jmssjournal.net on Sunday, January 31, 2021, IP: 10.232.74.23]

Short Communication

Real-Time Fast Fourier Transform-Based Notch Filter for Single-Frequency Noise Cancellation: Application to Electrocardiogram Signal Denoising

Anis Ben Slimane[1,2], Azza Ouled Zaid[3]

[1]Laboratory of Advanced Technology and Intelligent Systems, Sousse University, Sousse, [2]Department of Industrial Electronics, National Engineering School of Sousse, Sousse University, [3]SysCom Laboratory, National Engineering School of Tunis, University of Tunis EI Manar, Tunis, Tunisia

Abstract

Despite the considerable improvement of the common-mode rejection ratio of digital filtering techniques, the electrocardiogram (ECG) traces recorded by commercialized devices are still contaminated by residual power line interference (PLI). In this study, we address this issue by proposing a novel real-time filter adapted to single-frequency noise cancellation and automatic power line frequency detection. The filtering process is principally based on a point-by-point fast Fourier transform and a judicious choice of the analysis window length. Intensive experiments conducted on real and synthetic signals have shown that our filtering method offers very clean ECGs, due to the suppression of spikes corresponding to the PLI and the preservation of spikes outside the filter band. In addition, this method is characterized by its low computational complexity which makes it suitable for real-time cleaning of ECG signals and thus can serve for more accurate diagnosis in computer-based automated cardiac system.

Keywords: *Frequency detection, notch filter, physiological signals, power line interference removal, real-time fast Fourier transform, spectral filtering*

Submitted: 05-Jan-2020 **Revised:** 16-Feb-2020 **Accepted:** 26-Jul-2020 **Published:** 30-Jan-2021

Introduction

Electrocardiogram (ECG) is the oldest and most widely available physiological test. It allows identifying cardiovascular diseases (CVDs) while being entirely painless.[1]

A clean ECG is often required for the proper treatment of cardiac ailments. However, in a real scenario, the ECG signal is typically contaminated by different kinds of noises during its acquisition and transmission, such as the high-frequency noise (additive white Gaussian noise and power line interference [PLI]) and the low-frequency noise (baseline wandering).[2,3] Particularly, PLI noise causes a precision issue when interpreting low-amplitude waveforms like the ECG. In order to avoid the wrong identification of the characteristics of ECG signals and their impact on diagnostic accuracy, several PLI removal techniques have been developed.[4-7]

In this work, we propose a novel filtering method which has the particularity of eliminating noise with a single quasi-invariant frequency as it is the case for PLI. First, a point-by-point windowed fast Fourier transform (FFT) with an appropriate choice of the analysis window size is applied on the original ECG signal to accurately estimate the instantaneous amplitude value of PLI (50 Hz or 60 Hz). Finally, the instantaneous value of the filtered signal is determined by simply subtracting the computed noise value from the instantaneous value of the noisy ECG signal.

It is worth noting that the suggested method allows both the automatic detection and instantaneous suppression of PLI even in the presence of a variable noise amplitude. The simulation results have shown that the spectral response is stable and has a very narrow band rejection, ensuring a minimum of 33 dB attenuation in the band (49.8 Hz, 50.2 Hz). Moreover, the theoretical basis of the proposed denoising technique has been studied in addition to the relationship between the length of the analysis window and the filter parameter setting.

Always as part of experimental analysis, the simulation tests have been firstly conducted on synthetic ECG waveforms

This is an open access journal, and articles are distributed under the terms of the Creative Commons Attribution-NonCommercial-ShareAlike 4.0 License, which allows others to remix, tweak, and build upon the work non-commercially, as long as appropriate credit is given and the new creations are licensed under the identical terms.

For reprints contact: WKHLRPMedknow_reprints@wolterskluwer.com

How to cite this article: Slimane AB, Zaid AO. Real-time fast Fourier transform-based notch filter for single-frequency noise cancellation: Application to electrocardiogram signal denoising. J Med Sign Sens 2021;11:52-61.

Address for correspondence:
Dr. Anis Ben Slimane, Laboratory of Advanced Technology and Intelligent Systems, Sousse University, Tunisia, National Engineering School of Sousse, Sousse University, Sousse, Tunisia.
E-mail: bslimanea@yahoo.fr

Access this article online

Website: www.jmssjournal.net

DOI: 10.4103/jmss.JMSS_3_20

Quick Response Code:

[Downloaded free from http://www.jmssjournal.net on Sunday, January 31, 2021, IP: 10.232.74.23]

with a constant PLI amplitude. Thereafter, the same tests have been carried out with variable PLI amplitudes to determine the limitations of the proposed method. Finally, the experiments have been conducted on real ECG signals to compare their spectrums before and after filtering. According to the obtained results, it has been demonstrated that our filtering method delivers an impressive ECG quality, which is confirmed by the suppression of PLI spikes while preserving those outside the filter band in the frequency domain.

Background

The ECG consists of an electrical signal generated by the heart's muscular activity. Its graphical representation is commonly used to identify CVDs. However, in real-life scenarios, the recorded ECG signal is often corrupted with different types of noise: those caused by breathing, which generates a deflection of the isoelectric line;[8] those caused by the electrical activity of the muscle, which is also called electromyogram;[9] and those caused by PLI,[10] which is our focus. Previous studies showed the PLI noise with a frequency of 50 Hz or 60 Hz. This frequency has been subject to variations that do not exceed 0.5 Hz.[11,12]

Even though modern instrumentation amplifiers/differential amplifiers have a high common-mode rejection ratio, which attains 120 dB, the ECG recordings are still contaminated by PLI. In order to prevent the wrong identification of the ECG characteristics and its impact on diagnostic interpretation, advanced ECG denoising methods have been investigated. The most common solution is based on wavelet decomposition. The wavelet family is vital for the success of signal *denoising applications*, but wavelet-based notch filters cannot completely cancel PLI. Indeed, the residual traces may interfere with the ECG waves (P, Q, R, S, and T), make the detection of their onsets and offsets difficult,[13-16] and corrupt the proper function of automatic ECG analysis. Interference can also disturb the correct measurement of the RR interval (heart rate).[17]

Traditional analog and digital filters are not very selective and have the drawback of reducing or suppressing the ECG components near the power line frequency. Despite their limitations, different types of digital notch filters are still used.[17-19] To avoid affecting the signal components near the power line frequency, the cutoff band must be narrow, which leads to inefficient filtering with significant power line frequency deviation. Moreover, the resulting transient time is often unacceptably long.

PLI may be suppressed by adaptive filtering approaches.[20-24] However, this may be paid by a large transient response time.[17] Moreover, adaptive and nonadaptive notch filters introduce significant distortions in the QRS and ST-segment portions.[25] Soo-Chang and Chien-Cheng[18] tried to reduce the convergence time using a vector projection to find better initial values for infinite impulse response band-stop filters. Yoo *et al*.[19] put forward an adaptive central frequency hardware notch filter to track the frequency changes in the power line, thus reducing the bandwidth size. According to the results presented in Yoo *et al*.'s study,[19] the signal distortion cannot be adequately evaluated because of the small size of the used examples.

The Fourier decomposition method proposed in Singh *et al*.'s study[26] was an adaptive signal decomposition method that used the Fourier theory and aimed to remove baseline wander (BLW) and PLI. It could be considered as an adaptive and spectral denoising method. The experiments were done on real-life ECG data with synthetic BLW and PLI noise. In the best cases, the signal-to-noise ratio (SNR) did not exceed 15 dB.

Some methods have presented a lack of completeness, such that the authors have not shown the effectiveness of their denoising algorithms clearly enough in order to use them for PLI removal. In other methods, sometimes, the original signal has not been provided.[17,27] This is to say that no differences between original and processed signals are shown[28] and that the performance is only measured as a function of the mean square error instead of amplitude differences.

Methodology

Data collection

To evaluate the performance of the proposed technique, we have built a new database[29] using a wireless PC-based ECG device. By doing so, we have fixed the frequency sampling to 300 samples per second. The analog to digital conversion has been realized with the ADS1298 IC from Texas Instruments company, which is an eight-channel 24-bit ΔΣ simultaneous-sampling ADC.

For each subject, we have only recorded two limb leads (lead I and lead II) since lead III (aVR, aVL, and aVF) can be deducted automatically. The chest leads have not been collected. This database comprises one hundred subjects which have been collected by disabling the notch filter. This is to say that the recordings are contaminated with PLI at different levels.

Fast Fourier transform-based estimation of instantaneous power line amplitude

Fast Fourier transform basics

The Fourier transform Eq. (1) consists in representing a signal by a sum of sinusoids of frequencies and amplitudes as follows:

$$f_n = n\frac{F_S}{N} \quad A_n = \sum_{k=0}^{N-1} x_k e^{-\frac{2j\pi kn}{N}} \tag{1}$$

Where n is the frequency index, F_s is the sampling frequency, N is the number of samples, and A_n is the spike amplitude at frequency f_n.

[Downloaded free from http://www.jmssjournal.net on Sunday, January 31, 2021, IP: 10.232.74.23]

The value $f_1 = F_s/N$ is called the frequency resolution or the frequency step; it defines the fineness of the decomposition. The lower the value, the better the resolution.

Let us consider, for example, a sinusoidal signal of a frequency equal to 50 Hz, as for the power line, with an amplitude equal to 1. If this signal is sampled at a frequency F_e fixed to 300 Hz and the sample number N is equal to 100, then the frequency step will be equal to 3 Hz.

This means that we will get the amplitudes of the sinusoids of frequencies belonging to the set F = {0, 3,…, 297, 300}. In this case, we find that 50 Hz is not a part of this set. Accordingly, the signal will be distributed over a plurality of sinusoidal signals whose frequencies are the closest to 50 Hz. As depicted in Figure 1, the amplitude of these signals will tend to become weakened with an increasing distance from the signal frequency.

Finding the correct representation of this sinusoidal signal requires the 50 Hz frequency to be present on the X-axis; i.e., the 50 Hz frequency must be a multiple of the frequency step. By taking a window of 60 samples, the frequency step will be equal to 5 Hz, which is a divisor of 50 Hz. Accordingly, the signal will be represented by a single spike centered on the 50 Hz frequency whose amplitude is equal to 0.5 (half of the real amplitude), as shown in Figure 2.

We can deduce from this short analysis that it is possible to determine the amplitude of a sinusoidal signal embedded in another one through the Fourier transform.

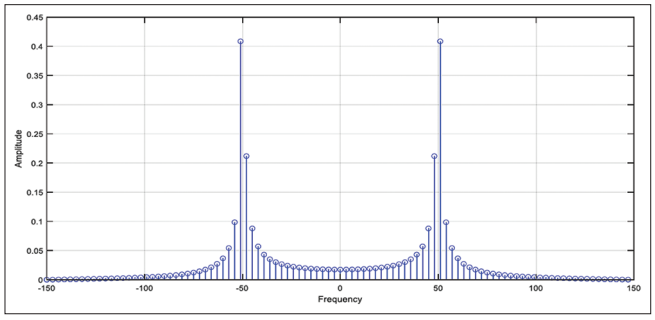

Figure 1: Graphical illustration of signal spectrum (f = 50 Hz, F_S = 300 Hz, and n = 100)

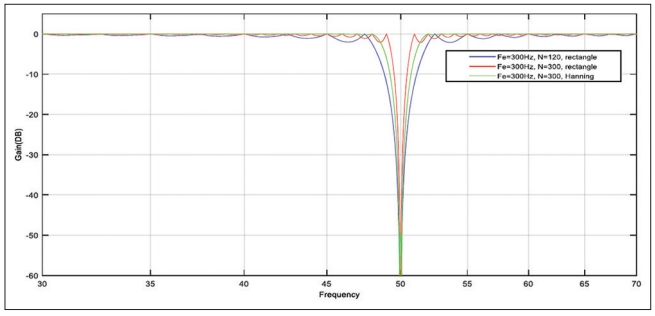

Figure 3: Effects of frequency resolution and window shape on filter response

Factors influencing filter parameters

In this section, we will determine the relationship between the frequency resolution $r = F_s/N$ and the filter cutoff frequencies. Therefore, we will vary the filter size N while maintaining the sampling frequency F_S = 300 Hz. The used window is the Hanning one. Using the rectangle window gives a response with an increase in the oscillation amplitude when approaching the cutoff frequency. The amplitude of oscillations decreases as the frequency resolution becomes finer. This concept is illustrated in Figure 3, whereas the corresponding zoomed version is depicted in Figure 4.

By varying the analysis window size N and preserving the sampling frequency F_s, the frequency resolution $r = F_s/N$ varies. When r varies, the high and low cutoff frequencies vary [Figure 4 for n = 120 and n = 300].

Figure 5 shows the relationship between the frequency resolution and the cutoff frequencies. By examining the two curves, we can clearly notice that the filter response is linear with the two parameters, which makes it easier to determine the cutoff frequencies if the frequency resolution is known, and vice versa.

Performance evaluation with respect to the power line interference amplitude

To adapt our method for real-time processing, an N-length shift register is used to store the last samples. A point-by-point FFT is then applied to this set of samples with instant processing.[30] To determine the interference

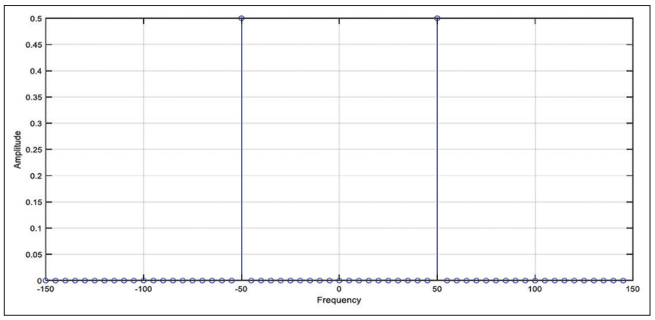

Figure 2: Graphical illustration of signal spectrum (f = 50 Hz, F_S = 300 Hz, and n = 60)

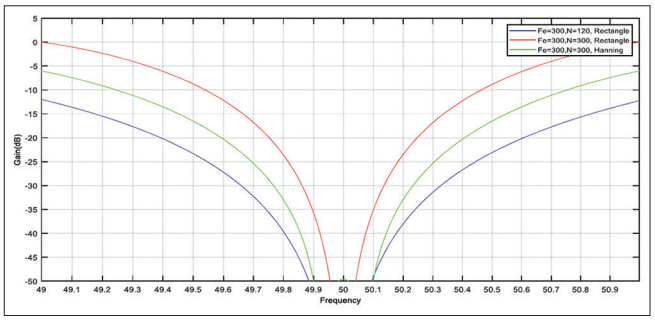

Figure 4: Effects of frequency resolution and window shape on filter response (zoomed plots)

[Downloaded free from http://www.jmssjournal.net on Sunday, January 31, 2021, IP: 10.232.74.23]

frequency, the spike amplitude corresponding to the 50 Hz is compared to that corresponding to the 60 Hz. It is worth noting that the power line frequency corresponds to the spike that has the highest amplitude.

Once the main frequency is set, the instantaneous value of the PLI amplitude can be subtracted from that of the noisy signal. This is expressed by Eq. (2):

$$\begin{cases} \hat{n} = \left|S(I)\right| cos\left(2 * pi\left(\frac{N-1}{2}\right) t_S + \varnothing\right) \\ \varnothing = atan\left(S(I)\right) \\ \hat{s} = s\left(t_e \frac{N-1}{2}\right) - \hat{n} \end{cases} \quad (2)$$

Where $\hat{n}$ is the estimated noise at the moment $t = t_s$ *(N –1)/2, s,* is the estimate of the denoised signal at the same moment *s*, is the noisy signal, *S* is the Fourier transform of *s,* and *I* is the spike index corresponding to the power line frequency which can be determined according to Eq. (3):

$$I = \frac{f_0}{r}, with\, r = \frac{F_S}{N} \quad (3)$$

Where f_0 is the PLI frequency (50 or 60 Hz) and *r* is the frequency resolution.

To obtain a fair value of the PLI amplitude, we have to multiply the amplitude value of the spike that corresponds to the noise frequency by 2. Then, we divide it by the area of the analysis window that corresponds to the average of its coefficients. It is worth pointing out that since the window is centered with respect to the sample index $\frac{N}{2}$, this technique will result in a time delay of about $t_S \frac{N}{2}$.

Moreover, the choice of the window size should be fixed according to the frequency variation in the power line amplitude. The higher the frequency variation is, the more reduced the window size must be. However, when filtering physiological signals such as ECGs, we are compelled to reduce the width of the stopband to remove only the interference and preserve the useful data. This reduction in the size of the stopband requires increasing the size of the window. A compromise between the bandwidth cutoff and the temporal localization should be considered. Notably, the automated choice of the analysis window size as a function of the frequency variation in the interference amplitude will be subject of future research work. Figure 6 represents the block diagram of the proposed filtering method.

To evaluate the performance of the proposed filtering technique, simulation tests have been conducted on two synthetic signals. The first one, "s_1" is expressed by Eq. (5). It consists of a sine wave "s" given by Eq. (4), which has been contaminated with the PLI of a constant amplitude. The second signal "s_2" is expressed by Eq. (6). It consists of the same sine wave "s" which, in turn, has been contaminated with the PLI of a variable amplitude. The graphical aspects of the two noisy signals are depicted in Figure 7.

$$s(t) = 0.5 sin\left(2\pi 1.25 t\right) \quad (4)$$

$$s_1(t) = \mathrm{s}(\mathrm{t}) + sin\left(2\pi 50 t\right) \quad (5)$$

$$s_2(t) = \mathrm{s}(\mathrm{t}) + \left(0.5 sin\left(2\pi \times 0.5 t\right) + 1\right) sin\left(2\pi 50 t\right) \quad (6)$$

We have tested the proposed technique using a 300-sample window, which corresponds to a 1 Hz frequency resolution and a stopband in the range of 48.75, 51.25 for F_S = 300 Hz [Figure 4].

Figure 8 depicts the filtering result when using the Hanning window on a noisy signal altered by PLI with a constant amplitude. From this figure, we can see a 0.5 s delay corresponding to half of the analysis window length. To calculate the value of the filtered signal at t = 0.5 s, samples belonging to the interval (0, 1) are required.

The SNR is expressed by:

$$SNR = 20 \log\left(\frac{\sum_{i=1}^{M} (o_i)^2}{\sum_{i=1}^{M} (o_i - f_i)^2}\right) \quad (7)$$

Where *o* is the original signal, *f* is the filtered one, and *M* is the number of signal components. This SNR has been

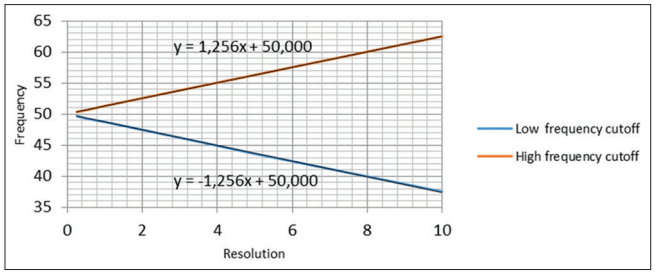

Figure 5: Graphical relationship between frequency resolution and cutoff frequencies

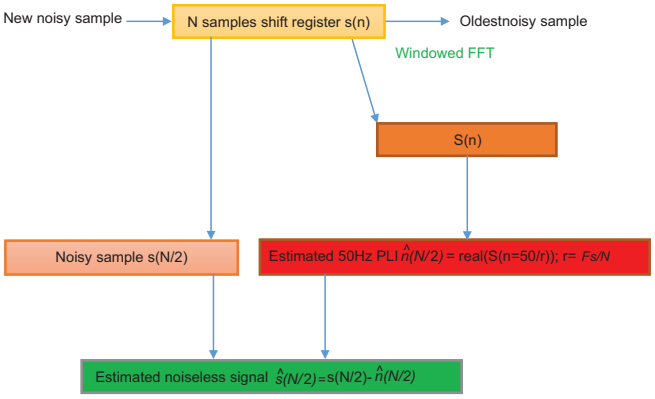

Figure 6: Block diagram of proposed method

[Downloaded free from http://www.jmssjournal.net on Sunday, January 31, 2021, IP: 10.232.74.23]

used to quantitatively compare the original signal to its filtered version. According to our experiments, the obtained SNR is equal to 217.0 dB.

Figure 9 shows the filtering result when using the Hanning window on two noisy signals, x_1 and x_2, with varied PLI. In both signals, the noise amplitude is the same. For the first signal, x_1, the frequency variation in the noise amplitude is equal to 0.5 Hz, whereas in the second signal, x_2 is equal to 0.25 Hz. After performing our filtering process on the two noisy signals, x_1 and x_2,

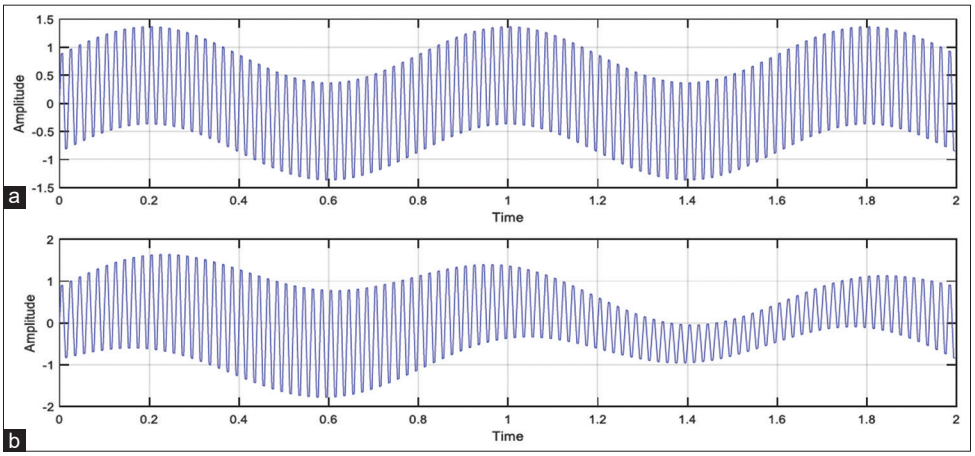

Figure 7: Graphical illustration of two simulated noisy signals: (a) "s_1" (b) "s_2"

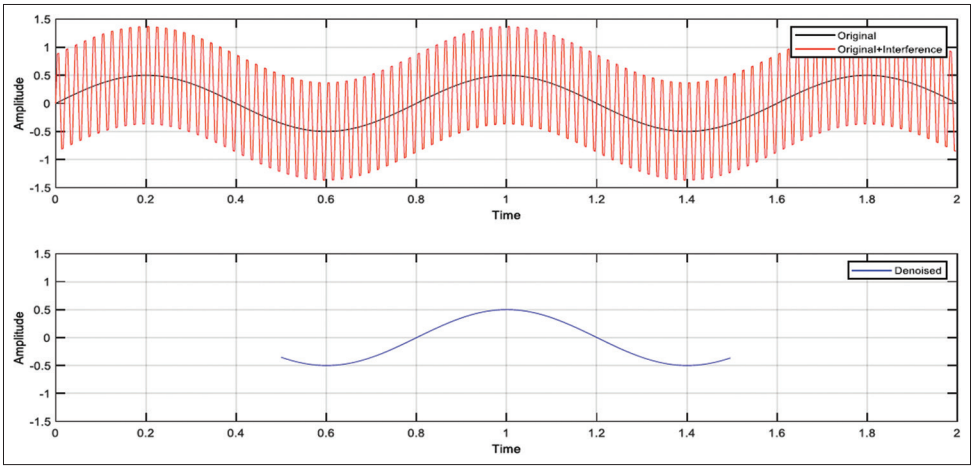

Figure 8: Graphical illustration of PLI removal in case of constant amplitude

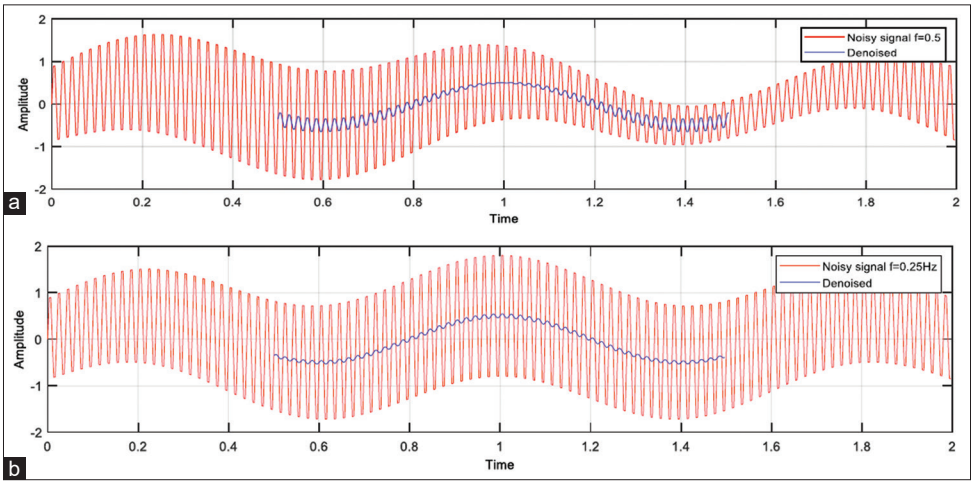

Figure 9: Graphical illustration of PLI removal in case of variable noise frequency: (a) *f* = 0.5, (b) *f* = 0.25

[Downloaded free from http://www.jmssjournal.net on Sunday, January 31, 2021, IP: 10.232.74.23]

we obtain an SNR value of about 39.8 dB and 58.7 dB, respectively.

It is clear that when the frequency of the noise amplitude increases, the determination of the instantaneous value of the noise becomes a difficult task. This is principally due to the fact that the analysis window has a temporal size of 1s. Thus, the interference amplitude varies several times along the window, which makes the determination of the instantaneous amplitude more difficult. This problem may be alleviated by reducing the size of the analysis window. However, this will be at the expense of the stopband width, which will be wider.

Experiments conducted on synthetic and real electrocardiogram signals

At this stage, we have conducted the first set of experiments on synthetic ECG signals to evaluate the performance of the proposed technique. Our choice has been justified by the fact that synthetic ECG signals allow a direct quantification of the difference between original and filtered signals.

The second set of experiments has been conducted on real ECG signals from our database.[29] For this kind of data, the performance evaluation is based on two criteria. The first one is a visual assessment of the quality of the filtered signal. The second criterion is quantitative. More specifically, we have proposed to carry out a quantitative assessment of PLI attenuation in the stopbands and a quantitative assessment of the conservation of ECG components outside the rejection bands.

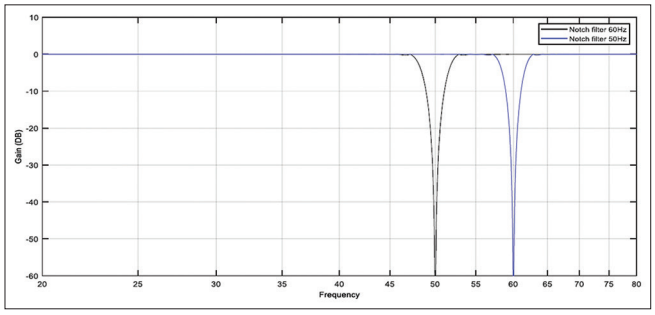

Figure 10: Filter response for *f* = 50 Hz and *f* = 60 Hz

Comparisons have been made with Butterworth and wavelet notch filters. The Butterworth filter[8] is set to a 4th order with a rejection band (49 Hz, 51 Hz), whereas for the wavelet-based filter, the algorithm suggested in Aqil and Jbari study[14] is used.

Since the power line frequency varies by ± 0.5 Hz, the size of the Hanning window is selected in a way that the minimum attenuation in the range of 49.5, 50.5 or 59.5, 60.5 is not less than 20 dB. The value of the window length that provides a step, which is a divisor of almost 50 and 60, ensures that minimum attenuation of 20 dB in the two intervals is 150. This value corresponds to a frequency resolution of 2 Hz and a stopband width equal to 2 × 2.512 Hz [Figure 5]. The filter responses are presented in Figure 10 for the two PLI frequencies: 50 Hz and 60 Hz.

The plots of the synthetic signal, the modeled noise *n* (expressed in Eq. 8), and the filtered signal are shown in Figure 11.

The synthetic is obtained with the NI LabVIEW Biomedical Toolkit. The sampling frequency is 300 Hz and the heart rate frequency is 60. The computed SNR for this simulation test is equal to 200.9 dB.

$$n = \left(0.25sin\left(2\pi \times 0.25t\right)+1\right)sin\left(2\pi 50t\right) \quad (8)$$

Figure 12 shows an example of the application of the proposed filtering technique on a real ECG signal extracted from our database.[29] Particularly, this trace corresponds to lead II. It is obtained by bringing an electric cord closer to the right arm electrode. This cord is connected to the 220 V 50 Hz mains. This permits obtaining a very noisy signal and consequently testing the limit of the proposed technique under extreme conditions.

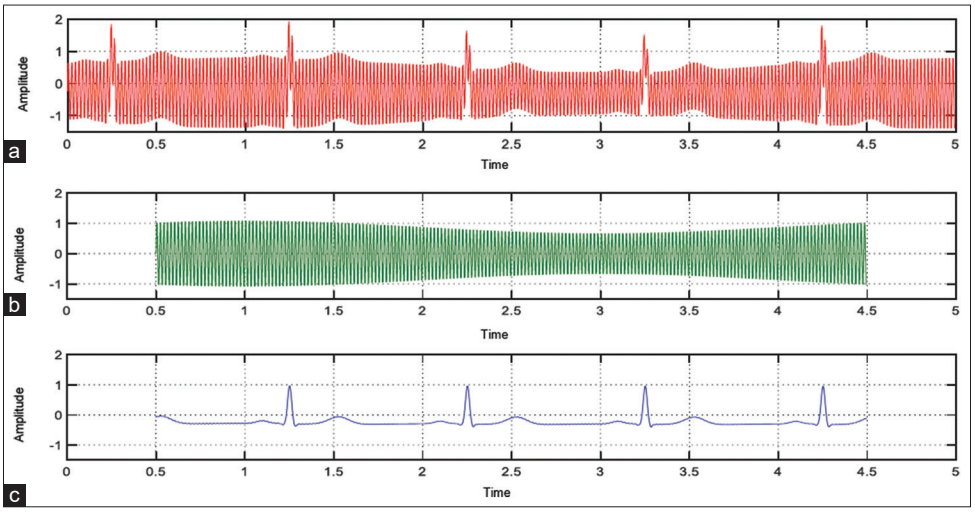

Figure 11: Graphical illustration of (a) synthetic noisy signal, (b) modeled noise, and (c) filtered electrocardiogram signal

[Downloaded free from http://www.jmssjournal.net on Sunday, January 31, 2021, IP: 10.232.74.23]

From Figures 12 and 13 (zoomed version), we can see a complete separation between the ECG waveform (blue) and PLI (green) whose peak-to-peak amplitude is almost twice that of the ECG waveform. This visual comparison, although appears very satisfactory, cannot, in any case, prove the selectivity of the filter.

For real signal filtering, the transfer function of the filter cannot be obtained (as it is the case of adaptive and wavelet-based filters). For this reason, we put forward the spectra comparison criteria, as illustrated in Figure 14. For greater accuracy, Figure 15 shows the zoomed version of the spectra of the noisy ECG signal and that of its filtered version, which is depicted in Figure 12.

From these spectra, we observe that the spikes corresponding to the PLI (located near the frequencies 50 Hz, 100 Hz, and 150 Hz) have been removed without affecting the other frequencies, which demonstrates the selectivity of the suggested filtering method.

To evaluate quantitatively the selectivity capability, we propose to assess the spikes amplitude attenuation on the rejection band and their conservation outside of the rejection band using the SNR metric.

As stated before, this metric is of great use if the transfer function of the filter cannot be determined.

In our experiments, we use an analysis window of length 300 (step = N/F_S), which corresponds to a frequency step equal to 1. According to the graphical relationship illustrated in Figure 5, the rejection band around 50 Hz is 48.74Hz, 51.26 Hz. Since we need to filter the 50 Hz multiple frequencies, the rejection bands (98.74 Hz, 101.26 Hz and 148.74 Hz, 150 Hz) should be considered as well.

Finally, to evaluate the noise cancellation, the SNR is computed only on the positive intervals (48.74 Hz, 51.26 Hz; 98.74 Hz, 101.26 Hz; and 148.74 Hz, 150 Hz). On the other side, to evaluate the signal conservation, the SNR is computed on the complementary intervals (0 Hz, 48.74 Hz; 51.26 Hz, 98.74 Hz; and 101.26 Hz, 150 Hz).

It is worth noting that outside the stopband, a high SNR value implies the good preservation of the signal components. Conversely, inside the stopband, the SNR

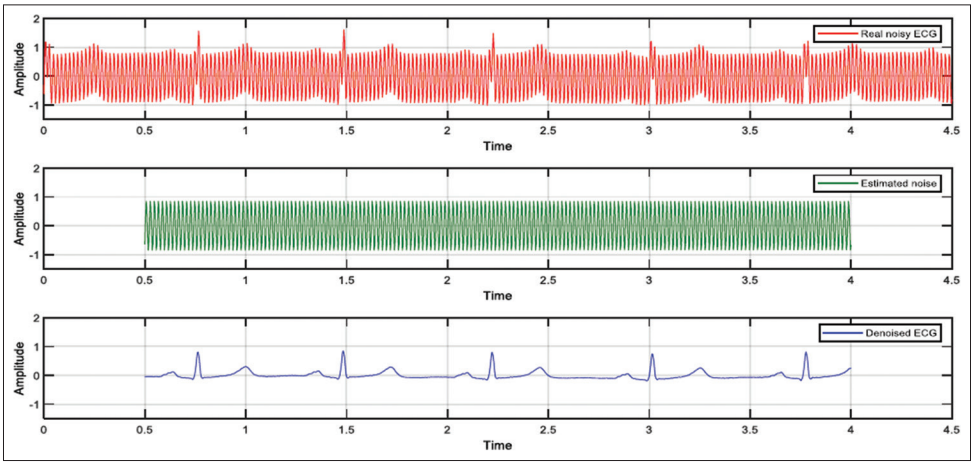

Figure 12: Graphical illustration of real electrocardiogram signal filtered with Hanning window (*n* = 300)

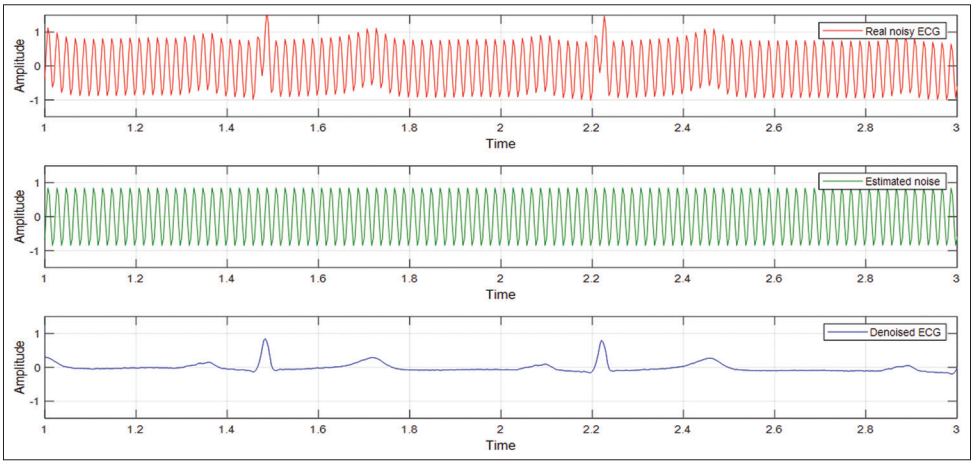

Figure 13: Graphical illustration of zoomed real electrocardiogram filtered with Hanning window (*n* = 300)

[Downloaded free from http://www.jmssjournal.net on Sunday, January 31, 2021, IP: 10.232.74.23]

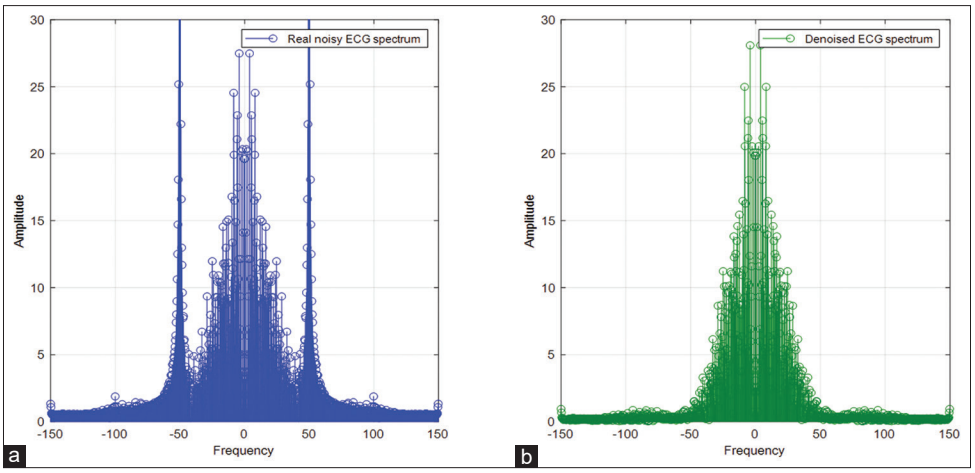

Figure 14: Spectrum of (a) original signal and (b) that of filtered signal using suggested method

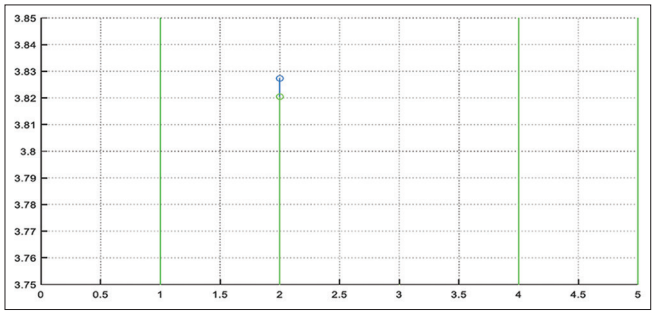

Figure 15: Zoomed spectrum of original signal and filtered one using proposed method

value must be as small as possible. In fact, a small value indicates good noise cancellation.

According to our experiments, the computed value of the SNR outside the stopband is equal to 70.9 dB, whereas that calculated inside the stopband is equal to − 51.6 dB. This value demonstrates the accurate selectivity of the proposed filter.

Finally, the suggested method is compared to the Butterworth and wavelet notch filters. Figure 16 shows the filtered signals for each method, and Table 1 provides the obtained SNRs.

From Table 1, we can see that all of the three methods can appropriately and identically remove PLI. Indeed, in the three cases, the SNR in the rejection band is approximately equal to − 51 dB. However, the proposed method has a better SNR outside the rejection band. This proves the filtering selectivity of the suggested method. Furthermore, and according to Figure 17, we can see a less perfect filtering quality obtained by the Butterworth and wavelet filters (presence of oscillations near the QRS waves) despite a quite similar SNR for the Butterworth filter compared to our method.

Conclusion

In this study, we have presented a real-time filter for single-frequency noise cancellation based on a point-by-point FFT. This method has the advantage of being effective in the presence of interference with variable amplitudes. Nevertheless, to effectively suppress interference, the period of the amplitude variation must be lower or equal to the extent of the analysis window. This hypothesis has been proved according to the tests conducted on the signals extracted from the created ECG database.

Table 1: Signal-to-noise ratio obtained for filtering methods

	SNR outside rejection band (dB)	SNR inside rejection band (dB)
Proposed method	70.9	−51.6
Butterworth	69.4	−51.1
Wavelet	13.4	−51.0

SNR: Signal-to-noise ratio

The proposed filter has a stable response and a very narrow cutoff band ensuring the minimal attenuation of 33dB in the band (49.8 Hz, 50.2 Hz).

Unlike the conventional filtering techniques which allow attenuating the noise amplitude in a well-defined band-stop, the suggested method can estimate the instantaneous power line amplitude with excellent accuracy and consequently allows suppressing it completely. Besides, we have determined the relationship between the frequency resolution and the cutoff frequencies of the notch filter to adapt the filter size according to the denoising requirements.

Experiments have been conducted on synthetic ECG signals affected with PLI with constant and variable amplitudes. Based on the experimental results, it has been shown that the proposed filtering method can effectively remove PLI without introducing significant distortions in the ECG waves (P, Q, R, S, and T). By considering real ECG signals, comparisons between noisy and filtered ECG spectra outside the rejection bands have given satisfactory results.

[Downloaded free from http://www.jmssjournal.net on Sunday, January 31, 2021, IP: 10.232.74.23]

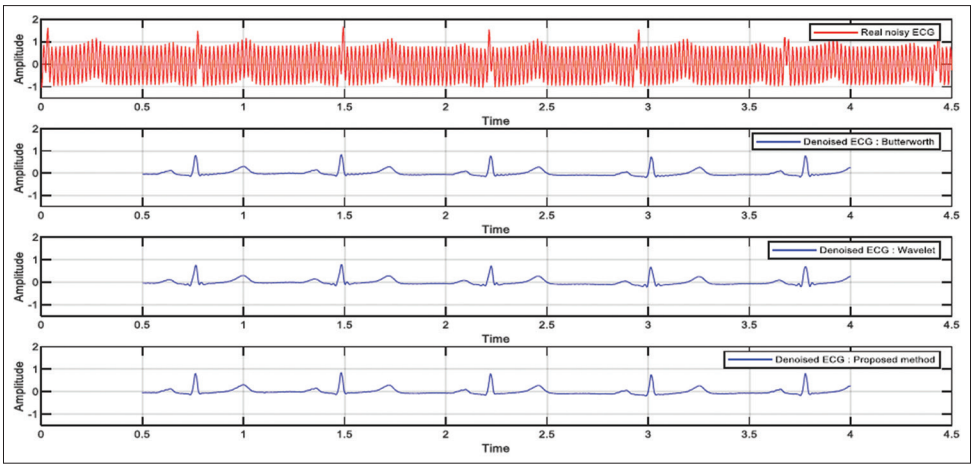

Figure 16: Denoising results for Butterworth, wavelet, and our method

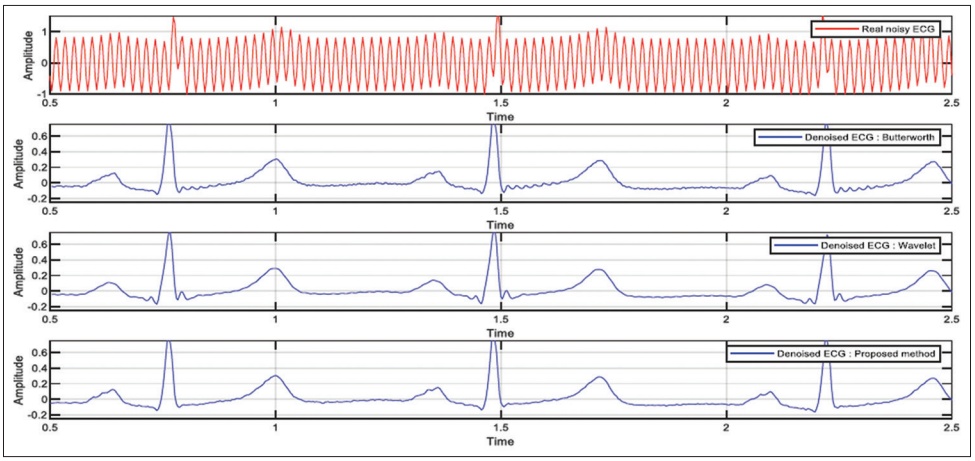

Figure 17: Denoising results for Butterworth, wavelet, and our method (zoomed version)

Comparisons between our method and two others showed a similarity on PLI rejection and a better signal preservation outside the rejection band for our method.

For the purpose of quantitative assessments, the use of the SNR metric is hampered by some serious limitations in the case of signals with fine *sensitive* structures. In our future work, we plan to alleviate this problem using an objective quality metric that takes into consideration the structural similarity.

Financial support and sponsorship

None.

Conflicts of interest

There are no conflicts of interest.

References

1. Biel L, Pettersson O, Philipson L, Wide P. ECG analysis: A new approach in human identification. IEEE Transac Instrumentat Meas 2001;50:808-12.
2. Lastre-Domínguez C, Shmaliy YS, Ibarra-Manzano O, Munoz-Minjares J, Morales-Mendoza LJ. ECG signal denoising and features extraction using unbiased FIR smoothing. Biomed Res Int 2019;2019: https://doi.org/10.1155/2019/2608547.
3. Rajesh KN, Dhuli R. Classification of ECG heartbeats using nonlinear decomposition methods and support vector machine. Comput Biol Med 2017;87:271-84.
4. Ziarani AK, Konrad A. A nonlinear adaptive method of elimination of power line interference in ECG signals. IEEE Trans Biomed Eng 2002;49:540-7.
5. Ladrova M, Martinek R, Jaros R. Power line interference elimination in ECG signals. J Biomimet Biomaterials Biomed Eng 2019;41:105-15.
6. Chen B, Li Y, Cao X, Sun W, He W. Removal of power line interference from ECG signals using adaptive notch filters of sharp resolution. IEEE Access 2019;7:150667–76. doi:10.1109/access.2019.2944027.
7. Singhal A, Singh P, Fatimah B, Pachori RB. An efficient removal of power-line interference and baseline wander from ECG signals by employing Fourier decomposition technique. Biomed Signal Proce Control 2020;57:, 101741. doi:10.1016/j.bspc.2019.101741.
8. Blanco-Velasco M, Weng B, Barner KE. ECG signal denoising and baseline wander correction based on the empirical mode decomposition. Comput Biol Med 2008;38:1-13.
9. Wu Y, Rangayyan RM, Ng SC. Cancellation of artifacts in ECG signals using a normalized adaptive neural filter. Conf Proc IEEE Eng Med Biol Soc 2007;2007:2552-5.

[Downloaded free from http://www.jmssjournal.net on Sunday, January 31, 2021, IP: 10.232.74.23]

10. Lehmann C, Reinstadtler J, Khawaja A. Detection of power-line interference in ECG signals using frequency-domain analysis. Comput Cardiol Confe Hangzhou 2011. p. 821-4.
11. Available from: http://electronics.stackexchange.com/questions/57878/how-precise-is-the-frequency-of-the-ac-electricity-network. [Last accessed on 2020 Jan 12].
12. Available from: https://www.nationalgrideso.com/balancing-data. [Last accessed on 2020 Jan 12].
13. Sahambi JS, Tandon SN, Bhatt RK. Quantitative analysis of errors due to power line interference and baseline drift in detection of onsets and offset in ECG using wavelets. Med Biol Eng Comput 1997;35:747-51.
14. Aqil M, Jbari A. Abdennasser bourouhou ECG signal denoising by discrete wavelet transform. Int J Online Biomed Eng 2017;13:51-68.
15. Ercelebi E. Electrocardiogram signals denoising using lifting-based discrete wavelet transform. Comput Biol Med 2004;34:479-93.
16. Ho CY, Ling BW, Wong TP, Chan AY, Tam PK. Fuzzy multiwavelet denoising on ECG signal. Electron Lett 2003;39:1163-4.
17. Levkov C, Mihov G, Ivanov R, Daskalov I, Christov I, Dotsinsky I. Removal of power-line interference from the ECG: A review of the subtraction procedure. Biomed Eng Online 2005;4:50.
18. Pei SC, Tseng CC. Elimination of AC interference in electrocardiogram using IIR notch filter with transient suppression. IEEE Trans Biomed Eng 1995;42:1128-32.
19. Yoo SK, Kim NH, Song JS, Lee TH, Kim KM. Simple self tuned notch filter in a bio-potential amplifier. Med Biol Eng Comput 1997;35:151-4.
20. Bensadoun Y, Raoof K, Novakov E. Elimination du 50 Hz du signal ECG par filtrage adaptatif multidimensionnel. Innovation 1994;15:750-9.
21. Ziarani AK, Konrad A. A nonlinear adaptive method of elimination of power line interference in ECG signals. IEEE Trans Biomed Eng 2002;49:540-7.
22. Wan H, Fu R, Shi L. The elimination of 50 Hz power line interference from ECG using a variable step size LMS adaptive filtering algorithm. Life Sci J 2006;3:90-3.
23. Thakor NV, Zhu YS. Applications of adaptive filtering to ECG analysis: Noise cancellation and arrhythmia detection. IEEE Trans Biomed Eng 1991;38:785-94.
24. Bellanger M. Digital Processing of Signals: Theory and Practice. USA: Wiley; 2000.
25. Hamilton PS. A comparison of adaptive and nonadaptive filters for reduction of power line interference in the ECG. IEEE Trans Biomed Eng 1996;43:105-9.
26. Singh P, Srivastava I, Singhal A, Gupta A. Baseline wander and power-line interference removal from ECG signals using Fourier decomposition method. Machine Intelligence and Signal Analysis.2018. p. 25-36. doi:10.1007/978-981-13-0923-6_3.
27. De Lima LA, Yioneyama T. A neural integrated circuit for noise cancellation in electrocardiograph signals. Proceedings of the 11th International Conference on Control Systems and Computer Science: Bucharest; 1997. p. 101-5.
28. Romanca M, Szabo W. Electrocardiogram pre-processing for the removal of high frequency and powerline frequency noise. Proceedings of the 6th International Conference on Optimization of Electrical and Electronic Equipments: Braşov; 1998. p. 703-6.
29. ECG Affected by50Hz Power Line Interference. Available from: http://www.eniso.rnu.tn; contact:Bslimanea@yahoo.fr. [Last accessed on 2019 Feb 03].
30. Available from: http://zone.ni.com/reference/en-XX/help/371361R-01/ptbypt/fft_ptbypt/. [Last accessed on 2020 Aug 28].